

# Effect of Processing Conditions on Dimensions of Sisal Fibers in Thermoplastic Biodegradable Composites

SALVATORE IANNACE, RAED ALI, LUIGI NICOLAIS

Institute of Composite Materials Technology (ITMC-CNR) & Department of Materials and Production Engineering, University of Naples "Federico II," Piazzale Tecchio 80, 80125 Naples, Italy

Received 14 February 2000; accepted 21 April 2000

**ABSTRACT:** Biodegradable composites based on treated and untreated sisal fiber and mater Bi-Z were processed using an internal batch mixer. The effect of processing conditions (temperature, speed of rotation, and time of mixing) and alkaline treatment on the dimensions of sisal fiber was studied. The length and diameter of the initial fibers were reduced during mixing and this effect was correlated to the magnitude of the shear stress developed in the mixer. An increase of the speed of rotation and/or a reduction of temperature produced fibers of smaller dimensions but with a higher aspect ratio  $l/d$ . Alkaline treatment increased the kinetics associated to the reduction of the fiber's dimensions. A semiempirical model was employed to predict the size of the fibers versus the time of mixing. © 2000 John Wiley & Sons, Inc. *J Appl Polym Sci* 79: 1084–1091, 2001

**Key words:** sisal fibers; lignocellulosic fibers; biodegradable composites; processing

## INTRODUCTION

In recent years, polymer composites containing natural fibers have received considerable attention in both the scientific literature and industry. Composites based on cellulosic fibers offer a number of benefits such as high stiffness and strength, desirable fiber aspect ratio, flexibility during processing with no harm to the equipment, low cost per unit volume, low specific mass, and good mechanical properties.<sup>1–3</sup> Cellulosic fibers are derived from renewable resources and have many desirable properties for reinforcement of thermoplastics such as low density, high stiffness, and low cost.<sup>3–8</sup>

Sisal fiber is one of the strongest fibers which can be used to produce reinforced polymeric materials for several applications. These fibers con-

tain about 78% of cellulose, 8% of lignin, 10% of hemicellulose and pectins, 2% of waxes, and 1% of ash.<sup>9</sup> Sisal fiber-reinforced composites show high impact strength besides moderate tensile and flexural properties compared to other cellulosic fibers.<sup>10</sup> However, the major drawbacks associated with the use of natural fibers as a reinforcement in thermoplastics are poor wettability and weak interfacial bonding with polymers. The use of coupling agents, pretreatment of fibers, grafting, and coating with suitable chemicals were reported to improve the interfacial adhesion between cellulosic fibers and thermoplastic matrices.<sup>11</sup>

The analysis of the effect of the processing conditions, during the preparation of the composites, on the fiber properties is a focal issue because many undesirable chemical reactions can take place as a consequence of high temperature, applied shear, and the presence of oxygen.<sup>12</sup> Thermal or oxidative fiber degradation will take place at high temperatures, for example, lignin starts

---

Correspondence to: S. Iannace.

*Journal of Applied Polymer Science*, Vol. 79, 1084–1091 (2001)  
© 2000 John Wiley & Sons, Inc.

to degrade at 200°C and most natural fibers start to lose strength at 160°C.<sup>4</sup>

Lignocellulosic fibers have been used with degradable and nondegradable polymers to reduce the cost of commodity thermoplastics. Most of the prior works on lignocellulosic fibers in thermoplastics deals with the use of wood flour and native cellulose fibers, such as kenaf, jute, flax, and sisal, with additives that can improve dispersion and interaction with the polymeric matrix. These composites show a higher elastic modulus but their strength is usually lower than that of the polymeric component due to the poor adhesion between the hydrophilic filler and the hydrophobic matrix. Fibers can work as reinforcement or as filler depending on the fiber/matrix interaction, on the aspect ratio, and on the critical fiber length. For this reason, it is very important to analyze the effect of the processing conditions (i.e., temperature profile, rheology, and residence time during extrusion) on the modification of the initial fiber length and diameter.

Lignocellulosic fibers have been used with nondegradable polymers, such as polypropylene,<sup>1,2,5,13</sup> polyethylene,<sup>4,7</sup> poly(vinyl chloride), and polystyrene<sup>14–16</sup> to reduce the cost of these commodity thermoplastics, but only few works have dealt with the effect of processing conditions on the properties of composites. In particular, Takase and Shiraishi<sup>13</sup> evaluated the effect of various kneading conditions (mixing temperature, rate of rotation, and mixing time) on the mechanical properties of a lignocellulosic fiber-based composite with polypropylene as the polymeric matrix. They showed that processing conditions influenced the breaking of the fibers and the final mechanical performances of the composites. Maldas et al.<sup>14</sup> studied the effect of mixing and molding temperatures on the mechanical properties of cellulosic fiber–polystyrene composites. They found that the mechanical properties of the composite decreased at temperatures above 200°C due to the degradation of some components of the fibers such as lignin and hemicellulose.

We reported on the preparation and characterization of biocomposites of a biodegradable matrix containing lignocellulosic fibers such sea algae fibers and sisal fibers.<sup>17,18</sup> Shear stresses developed in mixing and extrusion processes were responsible for damaging phenomena of the fibers and these effects are related to the different rheological properties of the thermoplastic matrices. Better mechanical properties were obtained in all those cases when a reduction of the diameter,

related to disgregation of the fibers, occurred while the aspect ratio  $l/d$  was preserved.

In this work, we analyzed the effect of process conditions on the statistical distribution of dimensions of sisal fiber after batch-mixing operations with biodegradable matrices. Fiber fragmentation and disgregation were modeled in order to correlate the reduction of fiber size and mixing time.

## EXPERIMENTAL

### Materials

Mater Bi-Z ZF03, supplied by Novamont (Italy), was used as the matrix. Sisal fibers, supplied by Brascordor (Brasil), were used either as-received and after alkaline treatment. The latter were prepared by placing the fibers in a stainless-steel vessel containing a 10% (w/v) solution of NaOH for 1 h at 80°C, under continuous stirring. Fibers were then washed in distilled water and oven-dried at 100°C until a constant weight was achieved.

### Mixing Operation and Fiber Extraction

A HAAKE Rheocord (Model 9000) was used to disperse the sisal fibers in the biodegradable polymeric melt. To simulate the effect of processing conditions, composites containing 20% sisal fibers were prepared at different temperatures, speeds of rotation, and mixing times. The fibers (initial average length equal to 5 mm) and the polymeric matrix were loaded together in the mix chamber at a low speed of rotation to reduce fiber degradation during loading operations.

The fibers were extracted from the composites by solubilizing the polymeric matrix in a mixture of dioxane and dimethyl sulfoxide at 60°C. After complete dissolution of the polymeric matrix, the solution was filtrated and the extracted fibers were dried in a vacuum oven at 60°C.

### Fibers Properties

#### Size

An optical microscope (Reichert–Jung) was used to measure the length and diameter of the dried fibers. Dimensions of 50 fibers were measured for each type of sample and they were statistically analyzed. Experimental data were elaborated to obtain the cumulative distribution function of the

fiber dimensions:  $F(d)$  for diameter,  $F(l)$  for length, and  $F(l/d)$  for the aspect ratio. The cumulative function  $F(x)$  describes the fraction of fibers having a dimension  $\leq x$ .

### Tensile Properties

Tensile testing of the fibers was carried out at room temperature using an Instron machine Model 4204 at a constant speed of 2 mm/min. Fifty fibers for each sample were used; the length of each fiber was 40 mm.

## RESULTS AND DISCUSSION

### Analysis of Fiber Properties

Short-fiber composites can be usually processed using processing technologies employed for thermoplastics. To achieve a good fiber dispersion in the polymeric melt, it is necessary to resort to the use of twin-screw extruders or to the use of mixing devices coupled to single-screw extruders. In both cases, the high shear stresses developed during mixing can result in the breakage of the fibers if the shear stresses transferred to the fibers overcome their tensile strength. Shear stresses result not only in the fragmentation of the fibers, but, for many lignocellulosic fibers, also induce their disgregation into fibers constituted by a discrete number of individual fibers, promoting an effective reduction of the average diameter of the reinforcing elements. These individual fibers are themselves composites of predominantly cellulose, lignin, and hemicellulose and their mechanical properties are dependant on the cellulose content and also on the angle at which fibrils are aligned in the fibers. Finally, the mechanical properties of the overall fiber is dependent on the properties of the matrix connecting the individual fibers, which usually is the weak link in the system.

To analyze the effect of temperature, speed of rotation, and mixing time on the damaging of sisal fibers, the statistical distribution of diameter  $d$ , length  $l$ , and aspect ratio  $l/d$  after processing was analyzed. Figure 1 shows the effect of the speed of rotation on the untreated sisal fiber size at 120°C. It can be clearly seen that an increase of the speed of rotation induced a reduction of both diameter [Fig. 1(a)] and length [Fig. 1(b)] and this is correlated to an increase of the shear stress, as shown by the increase of the mixing torque in

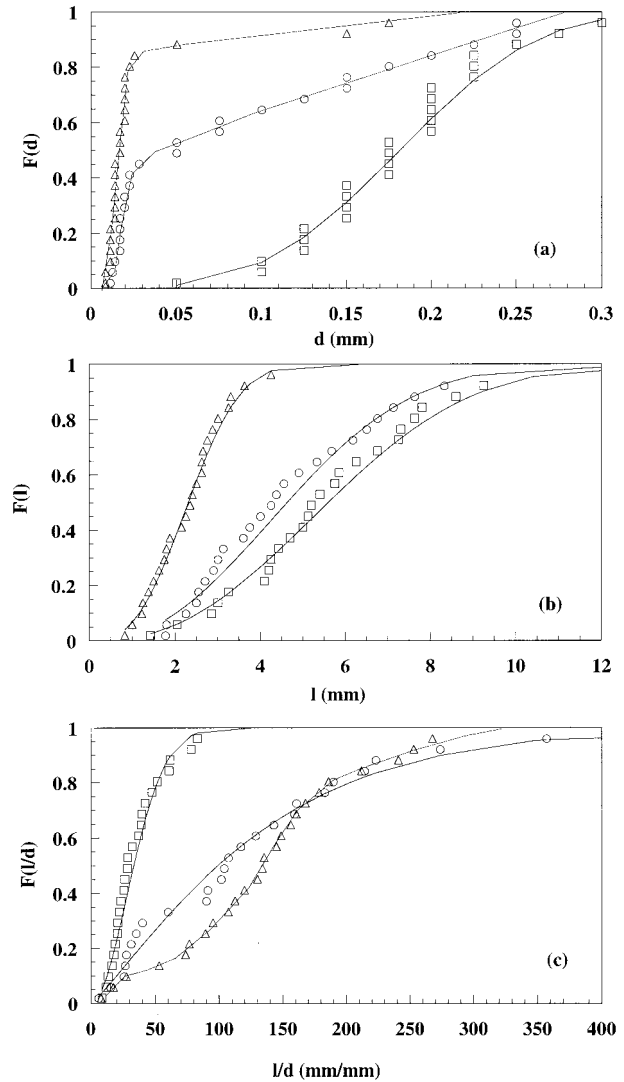


**Figure 1** Effect of speed of rotation on dimensions of untreated fibers ( $T = 120^\circ\text{C}$ ,  $t = 2$  min). Cumulative distributions of (a) diameter, (b) length, and (c) aspect ratio: (□) Before processing; (○) 50 rpm; (△) 150 rpm.

Figure 2. This is a positive result from a mechanical point of view, since reinforcing effects are correlated to the fiber aspect ratio  $l/d$ , which increases with increase of the speed of rotation, as shown in Figure 1(c).

Similar effects can be obtained if shear stress is modified by changing the mixing temperature with a constant speed of rotation. If temperature is reduced from 120 to 80°C (speed of rotation was 20 rpm), the increase of shear stress (see Fig. 2) resulted in higher fiber fragmentation and disgregation, as shown in Figure 3(a–c). Also, in this case, we observed an increase of  $l/d$  with increase of the mixing torque.

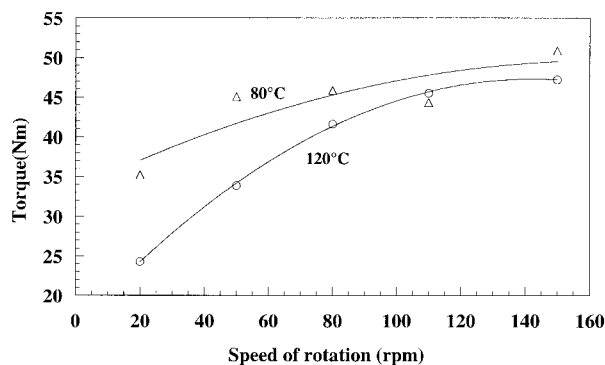


**Figure 2** Effect of speed of rotation and temperature on the average torque measured during mixing.

The alkaline treatment performed with the sisal fibers induced chemical and physical changes that affected the mechanical properties of the fibers. A statistical evaluation of the fiber strength was done on untreated and treated samples, and the results are compared in Figure 4.

The experimental data were analyzed by using the Weibull cumulative distribution function:

$$F(\sigma) = 1 - \exp\left[-\left(\frac{\sigma - \sigma_s}{\beta}\right)^\alpha\right] \quad (1)$$

where  $\alpha$ ,  $\beta$ , and  $\sigma_s$  are material constants related to the shape of the distribution, the mean value of stress, and the largest stress at which the probability of failure is zero, respectively. If  $\sigma_s$  is assumed to be equal to zero, the following values for  $\alpha$  and  $\beta$  were obtained:  $\alpha = 2.33$  and  $\beta = 243$  for treated fibers;  $\alpha = 1.95$  and  $\beta = 263$  for untreated fibers. These results indicate that the statistical distribution of the stress at break is wider for untreated fibers. The average strength of treated fibers is slightly lower than that of the untreated ones, and this is correlated to damaging effects due to the chemical reactions occurring during the alkaline treatment.

The lower strength displayed by the treated fibers does not have a remarkable effect on their length after processing. The cumulative distributions of length of treated and untreated fibers are compared in Figure 5 where the absolute values of  $d$ ,  $l$ , and  $l/d$  were normalized to the initial average values measured before the mixing procedures. Temperature, speed of rotation, and mixing time were the same in both experiments and the lower length displayed by the treated fibers shown in Figure 5(b) are, therefore, correlated to the different mechanical properties of the initial

fibers. This is due to the effect of treatment on cellulose which is converted from cellulose 1 to cellulose 2 and to the partial extraction of lignin and hemicellulose.<sup>16</sup> The latter can affect the properties of the individual fibers and, in particular, the extraction of the matrix components reduced the strength of the overall fiber to its disgregation in groups of individual fibers. This hypothesis is confirmed by the lower diameter of the treated fibers, as shown in Figure 5(a). Here, the difference in diameter is very small, since the time of processing (6 min) was too high to appreciate the effect of alkaline treatment. As discussed below, treatment induced a faster disgregation of the fibers, and it can be better observed

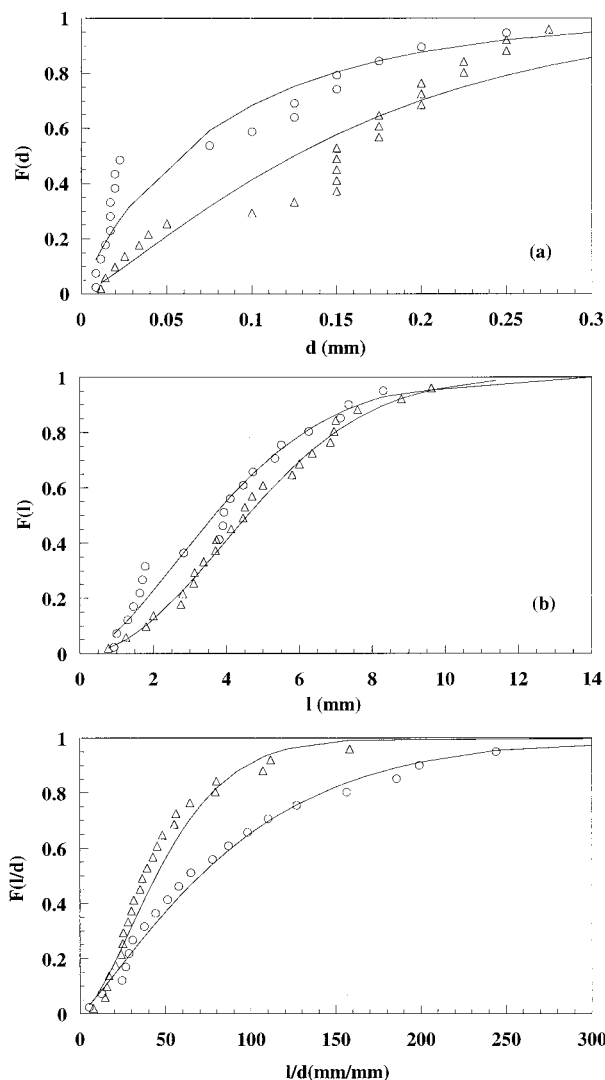


**Figure 3** Effect of temperature. Cumulative distributions of (a) diameter, (b) length, and (c) aspect ratio after 2 min at 20 rpm and (○) 80°C and (△) 120°C.

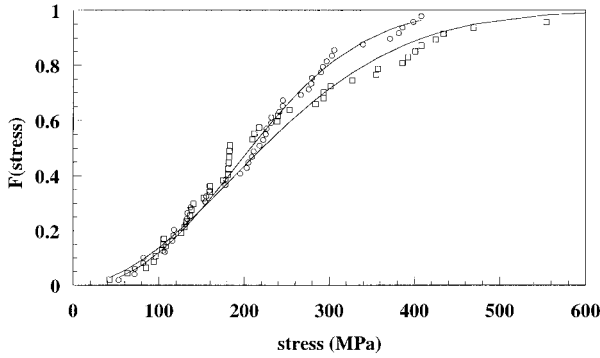


**Figure 4** Cumulative distributions of stress at break for (□) untreated and (○) treated fibers. Experimental data were fitted using the Weibull function and theoretical predictions are reported as continuous curves.

at a low time of mixing. As shown in Figure 5(c), only a slightly positive effect was obtained on the aspect ratio  $l/d$  after 6 min of mixing.

#### Effect of Time of Mixing and Theoretical Analysis

The effect of time of mixing on the dimensions of sisal fiber is shown in Figure 6. Diameter, length, and aspect ratio are reported in terms of the ratio  $\langle P \rangle / \langle P_0 \rangle$  between the average values measured on processed fibers  $\langle P \rangle$  and the average value of the initial fibers  $\langle P_0 \rangle$ . The increase of mixing time produced, at the beginning, a strong reduction of both  $\langle d \rangle$  and  $\langle l \rangle$  followed, at a higher time of mixing, by an almost horizontal trend, where these values did not vary significantly. Also, in this case, treated fibers showed a faster reduction compared to untreated sisal fibers.

The increase of mixing time produced a positive effect on the aspect ratio, whose average value became twice higher than the aspect ratio of the fibers before the processing. This situation is reached after 4 min of processing on treated fibers and after 10 min on untreated fibers. The matrix extraction due to the alkaline treatment resulted in the reduction of time of mixing required to reach the maximum  $\langle l \rangle / \langle d \rangle$ . This result suggests that processing induces the same effects on treated and untreated sisal fibers and the main difference can be correlated to the kinetics of fiber fragmentation and disgregation.

An explanation of this behavior can be made if we model the fiber damage during mixing. Internal mixers have two geometric features: a narrow gap between the rotor wings and mixer wall and a larger space between the rotors. This space is assumed to be a well-mixed tank in which exten-

sive mixing takes place, while dispersive mixing occurs in the narrow gap under the wing. When a fiber enters the narrow gap, it will be broken into smaller fibers if the hydrodynamic forces exceed the fiber strength and/or the cohesive force between the individual fibers. In the following discussion, we assume that the fibers will break every time in two smaller fibers with the same shape and size, and we use the same approach described for the dispersion of particles agglomerates.<sup>19</sup>

During each pass through the narrow gap, a fraction of particles is broken; this fraction is a function of two dimensionless groups  $L/H$  and  $Z$ ,

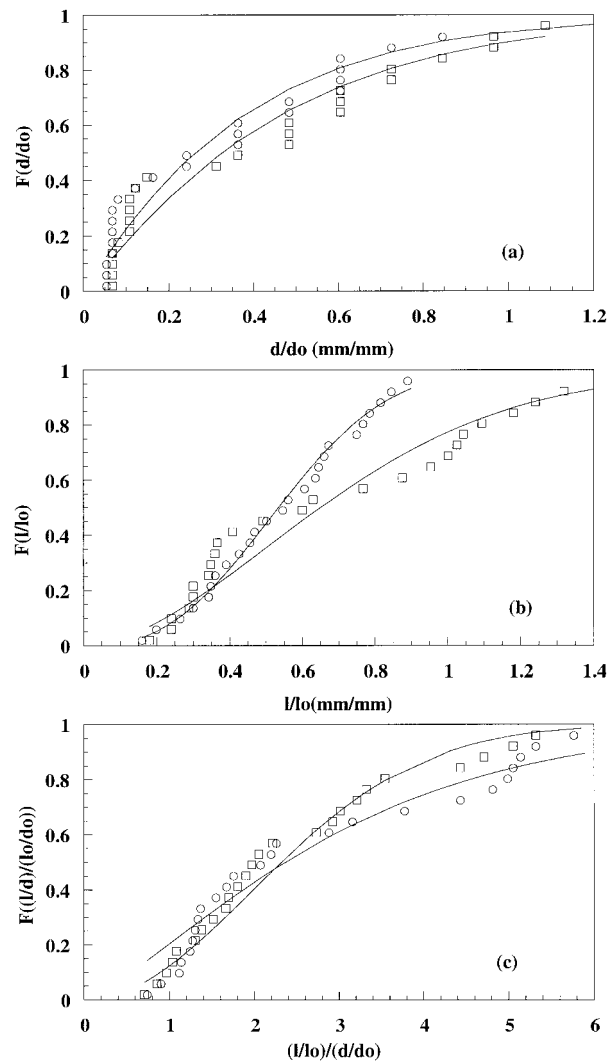


**Figure 5** Effect of fiber treatment on the statistical distribution of (a) diameter, (b) length, and (c) aspect ratio. Experimental data ( $T = 80^\circ\text{C}$ , 100 rpm,  $t = 6$  min) were normalized to the initial size of the fibers before processing: (○) treated; (□) untreated.

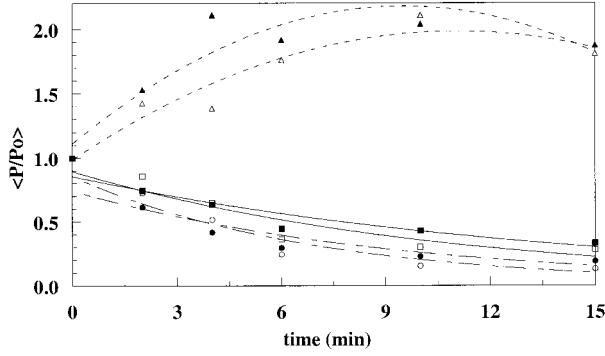


**Figure 6** Effect of mixing time ( $T = 120^\circ\text{C}$ , 100 rpm) on the variation of sisal fiber dimensions. Untreated fibers: ( $\square$ )  $d$ ; ( $\circ$ )  $l$ ; ( $\triangle$ )  $l/d$ ; treated fibers: ( $\blacksquare$ )  $d$ ; ( $\bullet$ )  $l$ ; ( $\blacktriangle$ )  $l/d$ .

where  $L$  and  $H$  are the gap length and height, respectively, while  $Z$  is a constant that depends on several factors such as the fiber shape and size, viscosity, and local shear rate. During mixing, the particles pass several times throughout the narrow gap, and the volume fraction of the fibers that have experimented  $k$  passes,  $G_k$ , is given by<sup>19</sup>

$$G_k = \frac{(t/t_1)^k e^{-t/t_1}}{k!} \quad (2)$$

where  $t$  is the mixing time, and  $t_1$ , the mean residence time in the well-mixed region.

In our case, when the fiber of size ( $l_0$ ) and ( $d_0$ ) enters the narrow gap, it will be broken to four fibers of size ( $l_1$ ) and ( $d_1$ ), then the new fibers will be broken to fibers of size ( $l_2$ ) and ( $d_2$ ), and so on. The size ratio between the fiber and its fragments is given by

$$\frac{l_i}{l_{i+1}} = 2, \quad \frac{d_i}{d_{i+1}} = 2 \quad (3)$$

The ratio between size of the fiber after ( $i$ ) ruptures and the initial fiber is given by

$$l_i = \frac{l_0}{2^i}, \quad d_i = \frac{d_0}{2^i} \quad (4)$$

When the fiber enters the narrow gap, rupture will occur, but after  $m$  passes, the size of the fiber will reach a critical value which equals the minimum size detected which was 0.025 mm for the diameter and 2.74 mm for the length. After  $k$  passes, the well-mixed region contains a distribu-

tion of small fibers of sizes  $l_i$  and  $d_i$ , where  $i$  varies from 0 to  $m$ .

After a given mixed time ( $t$ ), the well-mixed region consists of volume elements that have an experimental different number of passes in the high-shear zone, so the fraction of broken fibers ( $Y_m$ ) is given by.<sup>19</sup>

$$Y_m = 1 - \sum_{i=0}^{m-1} \frac{(at)^i}{i!} \times e^{-a \times t} \quad (5)$$

where  $a = X/t_1$  and  $X$  is the fraction of fibers that breaks during one pass through the narrow gap. Therefore, the fraction of unbroken fiber ( $Y$ ) will be

$$Y = 1 - Y_m = \sum_{i=0}^{m-1} \frac{(at)^i}{i!} \times e^{-a \times t} \quad (6)$$

The minimum average length and diameter of the smallest fibers ( $l = 2.734$  mm and  $d = 0.025$  mm) were experimentally evaluated after 15 min of mixing at  $120^\circ\text{C}$  and 100 rpm. The fraction of unbroken fibers ( $Y$ ) was evaluated from the experimental data reported in Figure 6, by normalizing the data in the following way:

$$Y = \frac{c - b}{1 - b} \quad (7)$$

where  $c$  is the experimental value of ( $l/l_0$ ) or ( $d/d_0$ ) after  $t$  min of mixing and  $b$  is the minimum ( $l/l_0$ ) or ( $d/d_0$ ) evaluated after 15 min of mixing.

The number of passes  $m$  required to reach the minimum values, which equal the size of the smallest fibrils, was 2 for length and 3 for diameter. The parameter  $a$  was obtained by fitting procedures on the experimental data and the best-fitting equations are reported below:

$$Y_1(d) = \left[ 1 + 0.9 \times t + \frac{(0.9 \times t)^2}{2} \right] \times e^{-0.9 \times t} \quad (8)$$

$$Y_2(d) = \left[ 1 + 0.875 \times t + \frac{(0.875 \times t)^2}{2} \right] \times e^{-0.0875 \times t} \quad (9)$$

$$Y_1(l) = (1 + 0.53 \times t) \times e^{-0.53 \times t} \quad (10)$$

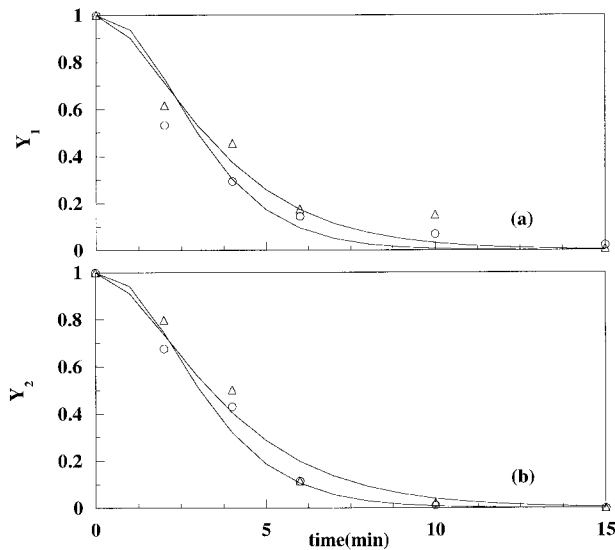


**Figure 7** Comparison between theoretical predictions [eqs. (9)–(12), continuous curves] and experimental fraction of unbroken fibers. (a) Treated and (b) untreated fibers: (○)  $d$ ; (△)  $l$ .

$$Y_2(l) = (1 + 0.5 \times t) \times e^{-0.5 \times t} \quad (11)$$

where  $Y(d)$  and  $Y(l)$  are related to a damaging analysis on diameter and on length. Pedices 1 and 2 indicate treated and untreated fibers, respectively. It is interesting to note that  $\alpha = x/t_1$  is always greater for treated fibers. This means that the fraction of broken fibers during each pass in the narrow gap is greater for treated fibers and this is again correlated to the lower mechanical properties of the fibers after treatment and to the partial extraction of the lignin matrix, as previously discussed.

The fraction of unbroken fibers predicted by eqs. (9)–(12) are compared to the experimental data in Figure 7. The good correlation between theoretical and experimental data indicates that the initial fiber is fragmented and disgregated into smaller fibers whose final dimensions, after a sufficient time of mixing, are not affected by the type of treatment employed on the initial fibers.

### Morphology

An SEM micrograph of the untreated and treated initial fibers is shown in Figures 8 and 9. Alkaline treatment removes organic compounds such as lignin and hemicellulose, leaving a smoother and cleaner surface [Fig. 8(b)] compared to the untreated fibers [Fig. 8(a)]. The presence of smaller individual fibers can be detected in both micro-

graphs. However, they are partially separated after the chemical treatment, and for this reason, disgregation effects during processing are favored.

Figure 9 shows sisal fibers processed at 120°C and 100 rpm. The individual fibers are still bonded together after 2 min [Fig. 9(a)] of mixing, but they are totally separated after 6 min [Fig. 9(b)] and this is attributed to the higher number of passes experienced by untreated fibers in the narrow gap. The alkaline treatment reduced the time needed for the complete separation of the single fibers, which occurred after only 2 min [Fig. 9(c)].

### CONCLUSIONS

Biodegradable composites based on sisal fibers and mater Bi-Z were prepared to study the effect

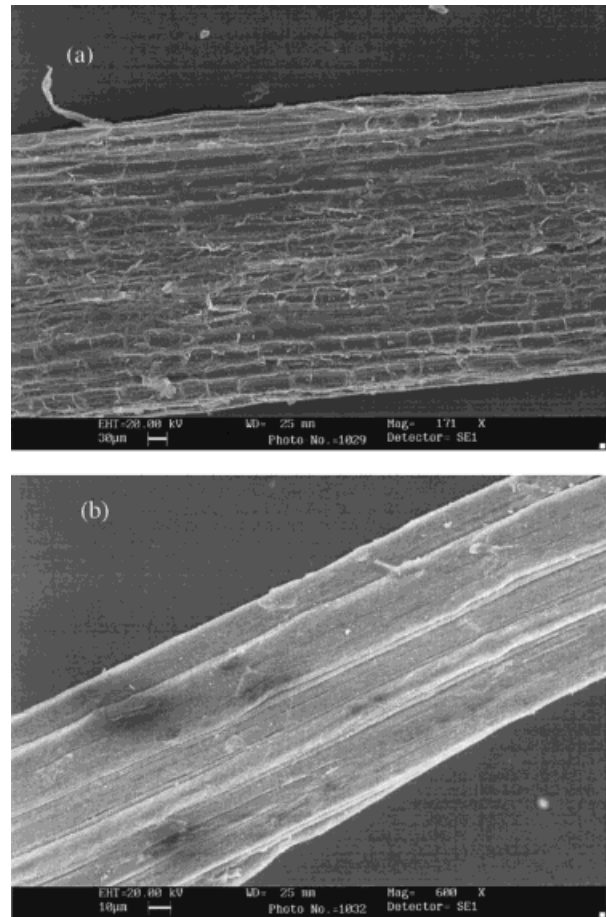


**Figure 8** SEM micrographs of (a) untreated and (b) treated sisal fibers before processing.

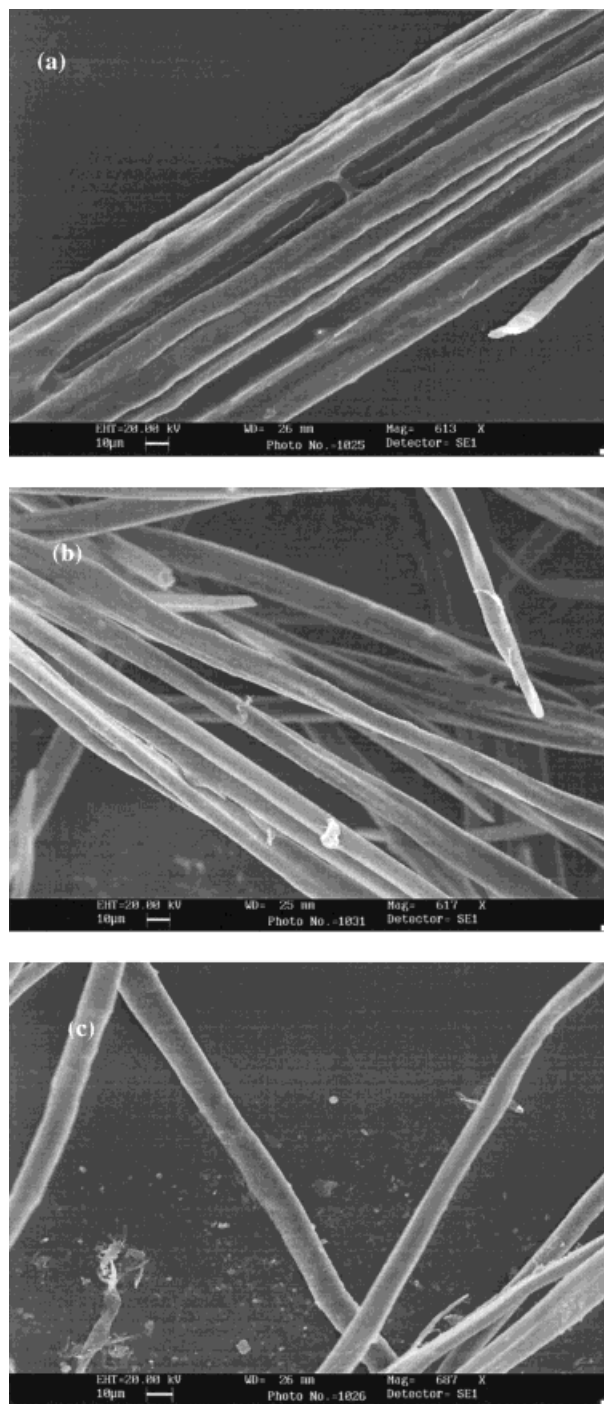


**Figure 9** Effect of mixing time and alkaline treatment on SEM morphology of sisal fibers processed at 120°C and 100 rpm. Untreated fibers: (a) 2 min and (b) 6 min; treated: (c) 2 min.

of processing conditions on fiber-size distributions. The length and diameter of the initial fibers were reduced during mixing and this effect was

correlated to the magnitude of the shear stress developed in the mixer. An increase of the speed of rotation and/or a reduction of temperature results in fibers of smaller dimensions but with a higher aspect ratio  $l/d$ . Alkaline treatment speeds up the process of fiber fragmentation and disgregation but do not affect the final dimensions after a sufficient time of mixing. Work is in progress to determine the effect of the size distribution on mechanical and viscoelastic properties of the composites.

## REFERENCES

- Gassan, J.; Bledzki, A. K. *Composites Part A* 1997, 28 A(12), 1001.
- Felix, J. M.; Gatenholm, P. *J Appl Polym Sci* 1991, 42, 609.
- Oksman, K.; Clemons, C. *J Appl Polym Sci* 1998, 67, 1503.
- Raj, R. G.; Kokta, B. V.; Madlas, D.; Daneault, C. *J Appl Polym Sci* 1989, 37, 1089.
- Park, B. D.; Balatinecz, J. J. *Polym Compos* 1997, 18, 79.
- Sandi, A. R.; Rowell, R. M.; Caulfield, D. F. *Polym News* 1996, 20, 7.
- Raj, R. G.; Kokta, B. V.; Maldas, D.; Daneault, C. *J Appl Polym Sci* 1991, 31, 1358.
- Yam, K. L.; Gogoi, B. K.; Lai, C. C.; Selke, S. E. *Polym Eng Sci* 1990, 30, 693.
- Mattos, L. H. C.; Ferreira, F. C.; Culvelo, A. A. S. *Lignocell Plast Compos* 1997, 241.
- Joseph, K.; Thomas, S.; Pavithran, C.; Brahakat, M. *J Appl Polym Sci* 1993, 47, 1731.
- Nair, K. C. M.; Diwan, S. M.; Thomas, S. *J Appl Polym Sci* 1996, 60, 1483.
- Al-Malaika, S. *Polym-Plast Technol Eng* 1990, 29, 73.
- Takase, S.; Shiraishi, N. *J Appl Polym Sci* 1989, 37, 645.
- Maldas, D.; Kokta, B. V.; Daneault, C. *J Appl Polym Sci* 1989, 37, 751.
- Czarnecki, L.; White, J. L. *J Appl Polym Sci* 1980, 25, 1217.
- Maldas, D.; Kokta, B. V. *Polym-Plast Technol Eng* 1990, 29, 119.
- Iannace, S.; Nocilla, G.; Nicolais, L. *J Appl Polym Sci* 1999, 73, 583.
- Vazquez, A.; Cyras, V. P.; Kenny, J. M.; Iannace, S. In *Proceedings of 12th International Conference on Composite Materials*, Paris, July 5–9, 1999.
- Manas-Zloczower, I. In *Mixing in Polymer Processing*; Rauwendaal, C., Ed.; Marcel Dekker: New York, 1991; Chapter 8.